RSC Advances

PAPER

View Article Online
View Journal | View Issue

Cite this: *RSC Adv.*, 2024, **14**, 21383

Photolysis of tolfenamic acid in aqueous and organic solvents: a kinetic study†

Sadia Hafeez Kazi,[a] Muhammad Ali Sheraz,[a] Zubair Anwar,*[b] Syed Ghulam Musharraf,[c] Sofia Ahmed,[a] Raheela Bano,[d] Tania Mirza,[b] Kyuyoung Heo[e] and Jun-Hee Na[f]

Tolfenamic acid (TA) is a non-steroidal anti-inflammatory drug that was studied for its photodegradation in aqueous (pH 2.0–12.0) and organic solvents (acetonitrile, methanol, ethanol, 1-propanol, 1-butanol). TA follows first-order kinetics for its photodegradation, and the apparent first-order rate constants (k_{obs}) are in the range of 0.65 (pH 12.0) to 6.94 × 10^{-2} (pH 3.0) min^{-1} in aqueous solution and 3.28 (1-butanol) to 7.69 × 10^{-4} (acetonitrile) min^{-1} in organic solvents. The rate-pH profile for TA photodegradation is an inverted V (∧) or V-top shape, indicating that the cationic form is more susceptible to acid hydrolysis than the anionic form of TA, which is less susceptible to alkaline hydrolysis. The fluorescence behavior of TA also exhibits a V-top-shaped curve, indicating maximum fluorescence intensity at pH 3.0. TA is highly stable at a pH range of 5.0–7.0, making it suitable for formulation development. In organic solvents, the photodegradation rate of TA increases with the solvent's dielectric constant and solvent acceptor number, indicating solute–solvent interactions. The values of k_{obs} decreased with increased viscosity of the solvents due to diffusion-controlled processes. The correlation between k_{obs} *versus* ionization potential and solvent density has also been established. A total of 17 photoproducts have been identified through LC-MS, of which nine have been reported for the first time. It has been confirmed through electron spin resonance (ESR) spectrometry that the excited singlet state of TA is converted into an excited triplet state through intersystem crossing, which results in an increased rate of photodegradation in acetonitrile.

Received 22nd February 2024
Accepted 27th June 2024

DOI: 10.1039/d4ra01369g

rsc.li/rsc-advances

Introduction

Tolfenamic acid (TA) belongs to the fenamate family of non-steroidal anti-inflammatory drugs (NSAIDs). It is used to treat various pain-related ailments in humans and animals.[1,2] Recently, its anti-Alzheimer effect[3–8] and anticancer activity against various cancers have also been identified and reported by many workers,[9–26] which have significantly increased its clinical importance.

TA (2-[(3-chloro-2-methylphenyl)amino]benzoic acid) is structurally similar to aminobenzoic acids and contains an amine group that is attached to the two benzoic acid rings (Fig. 1). TA is insoluble in water but soluble in dilute solutions of alkali hydroxides and most organic solvents.[1,27,28] It is a photosensitive drug known to degrade on exposure to UV/sunlight.[28–31] The most apparent result of photodegradation is the loss of the potency of the active drug and the formation of unwanted inactive products that may be toxic or harmful to the patients.[32] The literature lacks information regarding the photodegradation kinetics of TA in aqueous and organic solvents. No comprehensive investigations have been made for the photodegradation kinetics and the photoproducts formed thereafter. A couple of TA photodegradation studies performed

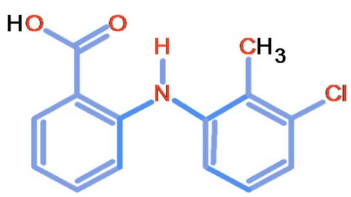

Fig. 1 Chemical structure of TA.

[a]*Department of Pharmaceutics, Baqai Institute of Pharmaceutical Sciences, Baqai Medical University, Karachi–75340, Pakistan*

[b]*Department of Pharmaceutical Chemistry, Baqai Institute of Pharmaceutical Sciences, Baqai Medical University, Karachi–75340, Pakistan. E-mail: zubair_ana@hotmail.com; zubair_ana@baqai.edu.pk*

[c]*Third World Center for Science and Technology, H.E.J. Research Institute of Chemistry, University of Karachi, Karachi–75270, Pakistan*

[d]*Dow College of Pharmacy, Dow University of Health Sciences (Ojha Campus), Karachi, Pakistan*

[e]*Reliability Assessment Center, Korea Research Institute of Chemical Technology, Daejeon 34114, Republic of Korea*

[f]*Department of Convergence System Engineering, Chungnam National University, Daejeon 34134, Republic of Korea*

† Electronic supplementary information (ESI) available. See DOI: https://doi.org/10.1039/d4ra01369g

earlier are related to the environmental effects of water pollution and toxicity.[29,30]

Since the literature lacks such information on TA, studying its photodegradation kinetics in aqueous and different protic and aprotic organic solvents could benefit pharmaceutical scientists, especially when its therapeutic uses have been repurposed. The information generated from the photostability studies would not only help to improve the medicinal stability of TA but would also help evaluate the handling and packaging aspects, therapeutic and adverse effects, and develop new drug delivery systems.[32] The present study has been carried out in aqueous media (pH 2.0–12.0) and some organic solvents (acetonitrile, methanol, ethanol, 1-propanol, 1-butanol) in which TA has been photodegraded by artificial UV light, and the reaction kinetics have been determined. The photoproducts have been identified, and a correlation has been established between the reaction rate, pH, and various physicochemical parameters of the solvents.

Experimental section

Materials

TA was obtained from Sigma Aldrich (St. Loius, MO, USA). Solvents and reagents used were of analytical grade purchased from BDH (Germany)/Merck (Germany)/DaeJung (Korea). The buffer systems used for the photolysis of TA were: KCl–HCl (pH 2.0), citric acid–Na_2HPO_4 (pH 3.0–8.0), H_3BO_3–KCl–NaOH (pH 9.0–10.0), and Na_2HPO_4–NaOH (pH 11.0–12.0). The ionic strength in each case was 0.02 M.

Methods

Thin-layer chromatography (TLC). TLC was carried out according to the method reported in British Pharmacopoeia[28] to confirm the purity of the active drug. Pure TA powder was weighed (25 mg) and dissolved in a mixture of methyl alcohol and methylene chloride in a 1 : 3 (v/v) ratio and diluted up to 10 mL of the same mixture. A 10 μL aliquot of the prepared solution was applied on precoated silica gel GF_{254} plates of 250 μm thickness (Merck, Germany). The TLC tank was equipped with a mobile phase containing a mixture of glacial acetic acid, dioxane, and toluene in a ratio of 1 : 25 : 90 (v/v). A stand-up time of 10 min was provided for saturation. The plate was then placed in the TLC tank to run in a mobile phase at 25 ± 2 °C. The plate was allowed to air dry, and the spot was observed under the UV lamp (Uvitech, Cambridge, UK) at 254 and 365 nm. Similarly, the results were reconfirmed by employing another method of TLC using hexane, chloroform, acetone, and glacial acetic acid in a ratio of 75 : 25 : 20 : 0.1 (v/v/v/v) as mobile phase at 25 ± 2 °C.[33] All protocols were followed in a similar pattern as described above.

FTIR spectroscopy. The powder sample of pure TA was analyzed using an FTIR spectrometer with ZnSE windows (Nicolet iS5, ThermoFisher Scientific, USA). The powder sample was placed on the diamond crystal optical base (iD7 ATR, ThermoFisher Scientific, Great Britain). The spectrum was collected at a 4 cm^{-1} resolution after performing 128 scans in the 4000–600 cm^{-1} region. The spectra were analyzed through Omnic software (version 9).

Spectrofluorimetry. The fluorescence measurements of TA in the pH range of 2.0–12.0 were carried out with a spectrofluorimeter (Jasco FP–8300, Japan) at room temperature (25 ± 2 °C) using 370 and 452 nm as excitation and emission wavelengths, respectively. A pure TA solution of 0.01 mM was used as a standard to measure the fluorescence intensity in relative fluorescence units.

NMR and mass spectrometry (MS). The purity of pure TA powder was ascertained by analyzing it through ^{1}H NMR spectrometry. The ^{1}H NMR spectra were recorded at 500 MHz (Avance AV-500, Bruker, Germany) using methanol (CD_3OD) as solvent.

The purity of TA was ascertained using electron ionization (EI) mass spectra in positive ionization mode (RT 1.5) using a heated probe (JEOL MS 600H-1, USA). The identification of the degradation products was made by analyzing the samples on UHPLC (Dionex Ultimate 3000, ThermoFisher, Germany) coupled with an Ultra High-Resolution QTOF mass spectrometer (Maxis II, Bruker Daltonics, Bremen, Germany) equipped with an electrospray ion source. The MS system was calibrated using an internal calibrant (sodium formate solution 0.01 M) injected at 3 μL min^{-1} using a syringe pump before each injection to ensure high mass accuracy. The separation was carried on an RP-18 column (100 × 3.0 mm, 1.8 μm, Macherey-Nagel, Düren, Germany). The column was maintained at 40 °C, and the injection volume was 10 μL. The flow rate of the mobile phase was 0.40 mL min^{-1}, solvent A was 0.1% formic acid, and B was methanol with 0.1% formic acid. All the samples were analyzed in positive ion mode. The parameters were set as follows:

The drying gas temperature was 270 °C, the flow of drying gas was set at 12.0 L min^{-1}, the capillary voltage of 4500 V, the mass range of 100–1200 *m*/*z*, the nebulizer pressure was set at 3.1 bar, the spectral rate was 2.00 Hz.

The same ion source conditions were also used for MS/MS mode. Data were recorded using Bruker Hystar software version 4.1 and calibrated using Data Analysis 4.4 (Bruker, Germany). Auto MS/MS analysis was done on pooled samples. The top 3 peaks were selected for MS/MS analysis with the active exclusion for 30 s.

The potential metabolite features were extracted, aligned, and intensity normalized on internal standard with data log2-transformed using Metaboscape 3.0 (Bruker, Germany). Metaboscape software was used for feature extraction using the following parameters: Intensity threshold 900 counts, minimum peak length 9 spectra, minimum peak length (recursive) 7 spectra, and minimum feature for extraction were 1/3 of all analyzed samples, including QCs. Features found less than 80% of samples were filtered. Every feature represents a specific *m*/*z* value of $[M + H]^+$ ion and possible sodium adducts, retention time, and peak height. For identification and molecular formula generation, exact masses of parent ions were matched with <5 ppm error and sigma value <50 in most cases. MS/MS spectra of significantly different features were searched

in NIST 14 Tandem Mass Spectral Library and Mass Bank of Europe.

Electron spin resonance (ESR) spectrometry. The spectra of TA (2.0 mg) in acetonitrile were recorded using an ESR spectrometer (JES-FA100, JEOL, Japan) equipped with a 500 W xenon lamp (SX-UI501XQ, Ushio, Japan).

pH measurements. The pH of the samples was set with the help of a digital pH meter (Elmetron CP501, Poland) using a glass electrode and a temperature probe. The instrument's calibration was performed using solutions prepared from commercially available buffer tablets of pH 4.0, 7.0, and 9.0 (Merck, Germany).

Assay of TA. It is of utmost importance to use an assay method that is accurate, precise, robust, and sensitive. However, it should also be stability-indicating to quantify the active drug in the presence of impurities and degradation products, particularly in kinetic studies. The HPLC method used in this study has previously been validated as per the guideline of ICH[34] and was found to be accurate, precise, robust, and stability-indicating with a t_R of 4.3 min.[31] All the photodegraded products identified through this method showed separate t_R from those of TA.

Radiation source. It is imperative to select an appropriate radiation source for the photolysis studies of any compound, as the experimental conditions are known to affect the degradation reactions significantly.[35] The photolysis rate depends on the experimental conditions, like the light source and its intensity; therefore, different visible and UV radiation sources are employed for such purposes.[35] An artificial UV light source has been used for the photolysis reactions in this study. The UV lamp emits maximum radiation in the UV-C region, *i.e.*, 254 nm, and partially (~5%) in the 300–550 nm regions. It is known to have a consistent UV output throughout its average life of 9000 h. It is effectively used in air and water disinfection units due to its constant UV output over its lifetime and is preferred for use in various photochemical processes. Such wavelength irradiation sources have been effectively employed for photolysis studies of different substituted aromatics,[36] including TA.[29] TA shows two absorption maxima in the 250–370 nm region.[27] Since the lamp emission is in the region of the studied drug; therefore, the photolysis reactions were performed with the same readily available radiation source. A previous study has also reported the photodegradation of TA in an alkaline solution with a similar wavelength lamp.[29]

Light intensity measurements. This actinometer developed by Parker[37] and Hatchard and Parker[38] is still considered the most useful actinometer over a wide range of wavelengths (254–577 nm) for determining light intensity. The irradiation of potassium ferrioxalate solutions in sulfuric acid results in the reduction of ferric to ferrous ions. The light intensity of the TUV light used in this study is found to be $5.62 \pm 0.12 \times 10^{18}$ qs^{-1}.

Photolysis

Aqueous solution. TA powder was solubilized in a few mL of ethanol, and its solutions (5.00×10^{-5} M) were prepared in the pH range of 2.0–12.0 using appropriate buffer systems. TA solutions were irradiated in the light chamber (Fig. S1†) with continuous stirring over the magnetic stirrer for constant light diffusion through the reaction vessels. Samples were withdrawn at regular intervals (0 to 180 min) and were subjected to the chromatographic assay.

Organic solvent. A stock solution of TA equivalent to 2.0×10^{-4} and 4.0×10^{-4} M was prepared separately in five different organic solvents, *i.e.*, methanol, ethanol, propanol, butanol, and acetonitrile. Each solution was transferred into the Pyrex reaction vessel and irradiated to UV light with constant stirring in the photolytic chamber. The drug was irradiated in each solvent for 96 h (4 days). The reaction vessels were marked for the solvent level, and the fresh solvent was added in case of any evaporation. The samples from the solution were withdrawn at different time intervals of 0, 6, 24, 30, 48, 54, 72, 78, and 96 h, and an appropriate dilution of 24 μg/10 mL was made in the mobile phase for the HPLC analysis. Each time, the dilution was filtered through a nylon membrane before the analysis. All experiments were performed in triplicate. Each blank solvent was also exposed to the UV light, as described above. Similarly, a set of drug samples in each solvent was stored in the dark in a tightly closed container to avoid evaporation.

Quantum yield of photolysis. The light intensity of Philips 30 W TUV was determined using a potassium ferrioxalate actinometer,[38] and the value was found to be $5.62 \pm 0.12 \times 10^{18}$ qs^{-1}. The amount of energy emitted by the irradiation source was calculated using the area under the respective emission band. These measurements were used to calculate the factor R, which gives the relation between the quantum number (Q_r) dissipated at the particular wavelength range (TA absorption bands) and the total quantum number (Q) found using potassium ferrioxalate actinometry. The absorbed quanta by TA were measured to calculate the quantum efficiency (ϕ). Hence:

$$A = K \times E_d$$

where A is the area (Sq. cm) under the emission bands, K is the constant that gives variations in the relative energy of the emission bands, and E_d is the energy emitted in the wavelength range covered by bands. The emission bands absorbed by TA (289, 338) to the total area of emission bands of the TUV tube were used to calculate the ratio (R).

$$R = \frac{A\lambda_1 + A\lambda_2}{A\lambda_1 + A\lambda_2 + A\lambda_3 + A\lambda_4 + A\lambda_5}$$

where λ_1, λ_2, λ_3, λ_4, and λ_5 are the wavelengths at 254, 313, 366, 405 and 436 nm, respectively.

The following relation was used to estimate the quantum efficiency (Φ) of TA:

The rate of photolysis $= K\ s^{-1}$ (initial concentration) $=$ moles s^{-1}

$$\varphi = \frac{\text{rate of TA photolysis (moles } s^{-1}) \times \text{no. of molecules per mole}}{R \times Q}$$

Result and discussion

Purity confirmation

TLC. The purity of the drug sample has further been ascertained by performing TLC according to the methods of British Pharmacopoeia[28] and Abdelwahab *et al.*[33] The results have been compared to that of the reference standard of TA. Both reference standard and sample spots appeared similar in position, color, and size (Fig. S2†), with a retention factor (R_f) of 0.8 and 0.49 by each method, respectively.

FTIR spectrometry. It is of utmost importance to confirm the purity of the active drug before validating the analytical method to ensure that there are no degrading products and unwanted impurities present in the sample that may interfere with the analysis. FTIR spectrometry has been performed to confirm the purity of TA. On comparing the sample with its reference standard, it was observed that there were no spectral changes between the two powders, which indicates that the material was pure and that no unwanted substances were present in the sample (Fig. S3†).

The characteristic stretching vibration of the amino group was detected in the region 3342–3340 cm^{-1}, while other characteristic peaks of the spectra were observed in the fingerprint region of 1661, 1582, 1500, 1440–1400, 1267, and 749 cm^{-1} for carbonyl, benzene ring, an amino group (bending vibration), a methyl group (symmetric stretching), C–H, and C–N deformation, respectively. All these peaks are in accordance with those reported in the literature for TA.[1,39–43]

NMR and MS. The data obtained through NMR and MS further confirmed the purity of the drug. EI-MS spectrum of TA showed the following peaks: *m*/*z* 261.0 (M^+, 63.7%), *m*/*z* 243.1 ($[M - 18]^+$, 55.1%), *m*/*z* 208.1 (100%), *m*/*z* 180.1 (22.5%), *m*/*z* 89.0 (6.4%), *m*/*z* 77.1 (5.7%), *m*/*z* 44.0 (4.0%). The *m*/*z* peaks obtained for TA through MS (Fig. S4†) are like those reported in the literature.[1]

The NMR spectrum of TA showed the following peaks: δ 7.97 (1H, dd, $J = 8$ Hz, 1.5 Hz, H-3), δ 6.72 (1H, t, $J = 8$ Hz, 1 Hz, H-4), δ 6.80 (1H, br d, $J = 8$ Hz, H-5), δ 7.26 (1H, dd, $J = 7.5$ Hz, 1.5 Hz, H-6), δ 7.14–7.31 (3H, m, H-4′, 5′, 6′), δ 2.295 (1H, s, CH_3). Similarly, the frequencies and intensities obtained for the sample in its ^{1}H NMR spectrum (Fig. S5†) are also found to be similar, thus confirming that the sample used was pure and potent.[1]

The purity of the active drug was ascertained before being subjected to photodegradation reactions. The purity of TA is confirmed by TLC (Fig. S2†), FTIR (Fig. S3†), MS (Fig. S4†), and NMR (Fig. S5†). Hence, before proceeding to the photodegradation reactions, it has been ensured that the drug is pure and that no prior degradation product(s) or additional impurities are present.

Kinetics of photodegradation in aqueous solution. TA concentrations in aqueous solutions after photodegradation reactions in the pH range of 2.0–12.0 obtained using HPLC assay method[31] are reported in Tables S1 and S2.† The initial concentration difference of TA in aqueous (5.00×10^{-5} M) and organic solvents (2.0×10^{-4} and 4.0×10^{-4} M) is due to its poor solubility in water. TA is practically insoluble in water;[1,28] therefore, it was dissolved in a few mL of ethanol before making its aqueous solutions at different pH. Due to this insolubility, it tends to precipitate at higher concentrations, particularly those used in organic solvents. Therefore, its photolysis reactions have been performed at lower concentrations in aqueous media than in organic solvents. The assay data obtained for the photolysis of TA were subjected to kinetic treatment, and it has been found that the TA follows first-order kinetics for its photodegradation in aqueous solutions (pH 2.0–12.0). The log concentration *versus* time plots at pH 2.0–12.0 are given in Fig. S6 and S7.† The apparent first-order rate constants (k_{obs}) were calculated from the slopes of the straight lines of the kinetic plots and are given in Table 1. First-order rate constants (k_{obs}) for the photodegradation of TA at pH 2.0–12.0 are in the range of 0.65×10^{-2} min^{-1} (pH 12.0) to 6.94×10^{-2} min^{-1} (pH 3.0) (Table 1).

Effect of pH. The effect of pH on photodegradation kinetics is essential in evaluating the stability of the drugs at a particular pH. Not much information in the literature is available regarding the pH effect on TA and its physicochemical properties. Various rate–pH profiles for the photodegradation of different drugs have been reported earlier.[44–47] A plot of k_{obs} *versus* pH for the photodegradation of TA has been constructed and found to be an inverted V ($\wedge$) or V-top shape (Fig. 2). The k_{obs}–pH profile for the photolysis of TA shows an increase in the rate constant from pH 2.0 to 3.0 (pK_{a1} 1.95)[43] with a maximum at pH 3.0, indicating that the cationic form of TA is more susceptible to acid hydrolysis. However, beyond pH 4.0 (pK_{a2} 4.05),[43] the rate of photolysis of TA decreases, and very low rate constants in the pH range of 6.0–12.0 have been observed (Table 1). It may be due to the low susceptibility of the anionic form of TA to alkaline hydrolysis. The V-top-shaped *k*–pH profiles have previously been reported for the hydrolysis of estrone phosphate,[48] dacarbazine,[49] hydrochlorothiazide,[50] tyrphostin,[51] 4-amino salicylic acid,[52] riboflavin[53,54] and piroxicam.[55]

TA shows a fluorescence emission band at 452 nm on excitation at 370 nm.[43] The correlation between fluorescence and the rate of photodegradation has been made by plotting the fluorescence intensity (A.U.) and the rate of photodegradation

Table 1 First-order rate constants (k_{obs}) for the photolysis of TA in the pH range 2.0–12.0[a]

pH	$k_{obs} \times 10^2 \pm$ SD (min^{-1})	R^2	t_{50} (min)	t_{90} (min)	ϕ
2.0	4.50 ± 0.22	0.9987	2.33	15.4	1.60
3.0	6.94 ± 0.34	0.9979	1.51	9.99	2.45
4.0	4.21 ± 0.51	0.9990	2.49	16.5	1.49
5.0	2.65 ± 0.19	0.9987	3.96	26.1	0.99
6.0	1.51 ± 0.29	0.9974	6.95	45.9	0.53
7.0	1.11 ± 0.44	0.9984	9.46	62.4	0.39
8.0	1.01 ± 0.18	0.9987	10.4	68.6	0.35
9.0	0.95 ± 0.55	0.9996	11.0	72.9	0.33
10.0	0.82 ± 0.36	0.9988	12.8	84.5	0.29
11.0	0.72 ± 0.69	0.9986	14.6	96.2	0.25
12.0	0.65 ± 0.58	0.9995	16.1	106.6	0.23

[a] ϕ = quantum yields of photolysis.

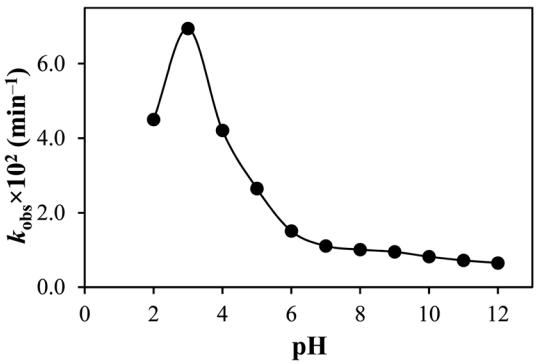

Fig. 2 The k_{obs}–pH profile for photolysis of TA in aqueous solution.

(k_{obs}) of TA *versus* pH (Fig. 3). It has been found that the fluorescence intensity (A.U.) *versus* pH is superimposed on the rate–pH profile. It indicates the maximum availability of the singlet excited state of TA at pH 3.0 and the minimum at pH range 7.0–12.0. Therefore, the photodegradation rate is higher at pH 3.0 than at pH 7.0–12.0, indicating the maximum formation of an excited triplet state at pH 3.0, resulting in the photodegradation of TA molecules. It has previously been reported that at higher pH values, the fluorescence of molecules is quenched and *vice versa*.[56,57]

Kinetics of photodegradation in organic solvents. The photodegradation of unionized molecules of TA has been carried out for 96 h (5760 min.) in five commonly used organic solvents, *i.e.*, acetonitrile, methanol, ethanol, 1-propanol, and 1-butanol. The molar concentration of TA in each solvent with time is given in Table S3,† and the degradation plots are shown in Fig. S8.† It has been observed that most of the degradation of TA (~50% or above) occurred in the initial 24 h (1440 min.) in most cases (Table S3†). However, it slowed down later, possibly due to the formation of photodegradation products and their interaction with the available photons. Similar patterns have also been reported previously for other drugs like riboflavin,[58–60] ascorbic acid,[61,62] and sulfacetamide.[63]

A curve pattern has been noted for TA molar concentration when plotted against the time in all solvents (Fig. S8†). Such a curve pattern indicates that the degradation does not follow zero-order kinetics. The log concentration of TA is determined from the molar recoveries, and first-order graphs have been plotted *versus* time (Fig. S9†). The plots indicated that the photolysis of TA in various organic solvents follows apparent first-order kinetics as a linear pattern against time has been observed (Fig. S9†). Such reactions indicate that the degradation products are formed from a constant fraction of the drug at a defined time following an unimolecular reaction.[45,58,64] The apparent first-order rate constants (k_{obs}) for the photodegradation of TA have been calculated from the slopes of the first-order plots by the following equation and are reported in Table 2.

$$k_{obs} = \frac{2.303}{t}\log\frac{a}{a-x}$$

where a is the initial concentration, and x is the amount that has changed in time, t. Therefore, if a, x, and t can be determined experimentally, k can be calculated in units of time. The rates (k_{obs}) for the photodegradation of TA in each solvent are between 4.13 to 7.69 × 10^4 min^{-1}, while the *R*-squared regression values are in the range of 0.986–0.996 (Table 2). The first-order rates obtained in the stability studies at various time intervals may represent a sum of rate constants for the photodegradation of multiple species.[58] Several drugs are known to follow first-order degradation kinetics, including riboflavin,[35,47,58–60] ascorbic acid,[61,64] cyanocobalamin,[62] methylcobalamin,[65] fluoroquinolones,[66–68] sulfacetamide,[63] *etc.* Among fenamates, various studies have also reported first-order degradation kinetics for drugs like mefenamic acid,[69–73] meclofenamic acid,[74] and also for TA.[29,30,75]

Effect of TA concentration on the photodegradation. Drug concentration plays a vital role in the degradation as it may affect the reaction rate.[61,76] Dilute solutions of drugs are known to be more prone to degradation than concentrated ones.[74,76,77] Therefore, the effect of TA concentration on the photodegradation rate has also been ascertained by exposing double-strength stock solution (*i.e.*, 4.0 × 10^{-4} M) in different organic solvents to the same intensity UV light under similar experimental conditions. The molar concentration of TA after photolysis in various organic solvents is reported in Table S4.† The comparative concentration *versus* time plots with respect to the original concentration (*i.e.*, 2.0 × 10^{-4} M) in each organic solvent is shown in Fig. S10.† The results indicated a similar curve pattern with slightly lower degradation rates (Table S4†) than the solutions containing a lesser amount of the drug (Table S3†).

Similarly, the k_{obs} values for the photolysis of TA in each solvent calculated from the first-order plots (Fig. S9†) are also found to be lesser, *i.e.*, 3.28 to 6.28 × 10^4 min^{-1}, with regression values of 0.984–0.995. The results indicated that 50% of the drug degradation (t_{50}) in double-strength solutions occurred in about 18–35 h (Table 2) compared to 15–28 h of original solutions (Table 2). The faster degradation rate of the solutions containing lower TA concentrations under similar photolysis conditions could be due to the availability of more photons for

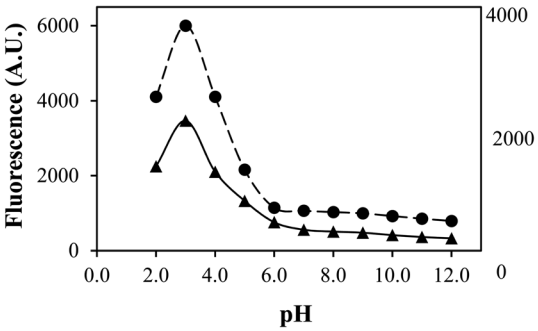

Fig. 3 *k*obs–pH profile (▲) for the photolysis of TA at pH 2.0–12.0, along with fluorescence intensity *versus* pH curve (●). The values of k_{obs} have been increased to 500 folds to match the fluorescence curve.

Table 2 Apparent first-order rate constants (k_{obs}) for the photodegradation of TA in different organic solvents with half (t_{50}) and shelf-life (t_{90})[a]

Solvent	Dielectric constant	Acceptor number	Viscosity (mPa s)	Ionization potential (eV)	Density (g mL^{-1})	Concentration (M × 10^4)	$k_{obs} \times 10^4 \pm$ SD (min^{-1})	R^2	t_{50} (h)	t_{90} (h)	Φ
Acetonitrile	38.5	18.9	0.369	12.20	0.777	2.00	7.69 ± 0.90	0.991	15.01	2.27	0.11
						4.00	6.28 ± 1.50	0.986	18.38	2.79	0.18
Methanol	32.6	41.3	0.544	10.84	0.787	2.00	6.48 ± 1.20	0.996	17.83	2.70	0.09
						4.00	5.54 ± 1.05	0.990	20.85	3.16	0.16
Ethanol	24.3	37.1	1.074	10.47	0.785	2.00	5.85 ± 1.35	0.994	19.73	2.99	0.08
						4.00	4.74 ± 1.25	0.995	24.37	3.69	0.13
1-Propanol	20.1	37.3	1.945	10.15	0.800	2.00	4.67 ± 0.75	0.990	24.73	3.75	0.07
						4.00	4.12 ± 0.88	0.987	28.05	4.25	0.12
1-Butanol	17.8	36.8	2.544	10.04	0.806	2.00	4.13 ± 0.80	0.986	27.97	4.24	0.06
						4.00	3.28 ± 1.10	0.984	35.26	5.34	0.09

[a] Φ quantum yields of photolysis.

the excitation of the TA molecule than the higher concentrations.

Effect of solvent. The effect of a solvent on a drug is a widely studied parameter due to its influence on the degradation rate. Depending upon the solute–solvent interaction, various solvent characteristics may directly or indirectly affect drug stabilization or degradation.[58,66–68,78–81] In the present study, four commonly used protic (alcohols) and a polar aprotic organic solvent (acetonitrile) have been employed to study their impact on the photodegradation of TA. The solvents have been selected based on their common lab usage, easy availability, and physicochemical characteristics like dielectric constant, viscosity, acceptor number, ionization potential, and density. The results indicated that the photolysis rate of TA is influenced by the nature of the solvent when irradiated under similar experimental conditions. Whether the drug solution was diluted or concentrated, the degradation rate is found to be in the following order (Table 2):

Acetonitrile > methanol > ethanol > propanol > butanol

Various physicochemical properties of the selected solvents (Table 2) have been correlated with the degradation rates to ascertain the multiple factors influencing the photodegradation of TA, which are discussed in the following sections.

Effect of solvent dielectric constant. The permittivity or dielectric constant (ε) of a solvent is a measure of its polarity. The dielectric constant of a solvent is often valuable for stabilizing a pharmaceutical formulation and is considered an essential parameter for predicting solute–solvent interactions.[45,47,58,78] Any change in the dielectric constant value of a solvent may alter the activation energy, thus affecting the degradation rates.[46,58,78,81] A correlation has been made between the apparent first-order rate constants of TA (Table 2) and the solvent dielectric constants (Table 2), and the plot is shown in Fig. 4.

The results indicated that the photodegradation of TA increased linearly with an increase in the dielectric constants of the solvents (Fig. 4). The increase in the degradation rate of TA with an increase in the solvent dielectric constant indicates that the reaction involves polar or similar charged degradation species; therefore, the rate has been accelerated in solvents having high ε values (Table 2). This pattern of enhanced degradation of TA with increasing dielectric constants is known to occur when identical charged species are involved in the reaction. On the contrary, the decrease in the degradation rate with an increase in dielectric constant often occurs when the reaction occurs between ions of opposite charges.[82–84]

A linear pattern was noted in the thermal degradation studies of TA when the dielectric constant was increased in the ethanol–water mixtures by increasing the amount of water.[75] A similar effect has also been observed previously in drugs like riboflavin,[58] fluoroquinolones,[66–68] and 5-fluorouracil.[81] Based on these findings, it is suggested that using a combination of appropriate solvents for TA may result in comparatively better stability.

Effect of solvent acceptor number. The rate of degradation of a drug is dependent on its electron-donating capacity, which is affected by the nature of the solvent.[58,85] The acceptor number (AN) is a benchmark for the solvents' capacity to share electron pairs with compatible donors. This property of solvents may affect the reaction or photolysis rate.[58,78,81] In the present study, a correlation has been made between the apparent first-order

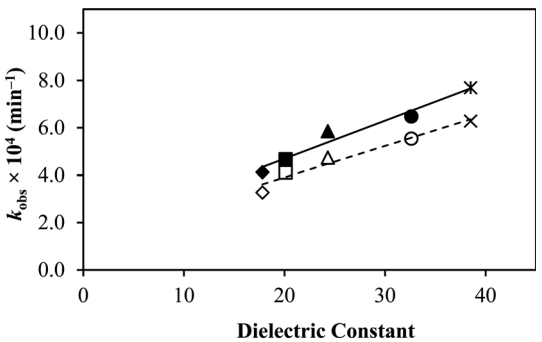

Fig. 4 A plot of k_{obs} of TA *versus* dielectric constant of the solvents. (*, ×) Acetonitrile, (●, ○) methanol, (▲, Δ) ethanol, (■, □) propanol, and (◆, ◇) butanol. (– – – –) 2.0 × 10^4 M; (– – – –) 4.0 × 10^4 M.

rate constants (k_{obs}) of TA (Table 2) and the AN of highly structured protic solvents, *i.e.*, above 25 (Table 2). The value of acetonitrile does not follow the pattern linearly, probably due to its different aprotic nature. At the same time, a somewhat linear pattern has been noted in the alcohols (Fig. 5). The increase in solvent AN of alcohols increased the photolysis rate, and hence, using a combination of solvents may reduce the degradation rates.

Effect of solvent viscosity. The viscosity of the solvents or media in which the drug is present is an essential intensive physical property that directly affects the drug stability and degradation rate. The literature holds ample evidence that the degradation rate can be altered for certain drugs by controlling the viscosity of the medium.[35,58,61,78,81,86] In the present study, when the viscosities of the solvents (Table 2) are plotted against the photolysis rates of TA (Table 2), a linear pattern has been obtained (Fig. 6). This linearity thus indicates that the increase in the viscosity of the solvents resulted in a decrease in the photolysis of TA. The increase in the viscosity could have resulted in lesser penetration of the UV light in the medium, thus causing a reduction in the rate of degradation of TA.

A correlation between the effect of solvent viscosity on the rates and mechanism of chemical reactions with certain drugs has been reported.[35,58,61,78,81,86–88] A similar viscosity effect was observed when the photodegradation of fenamates was found to lower with an increase in medium viscosity.[89,90] The temperature of the medium plays a vital role in the viscosity effect on the reaction rate.[84] The opposite result has been observed in the case of the thermal degradation of TA in ethanol–water mixtures. It was observed that the increase in the viscosity of the medium resulted in increased degradation of TA due to a rise in the temperature.[75]

Effect of solvent ionization potential. The ionization potential of a solvent is the minimum energy required to remove an electron from the molecule of that solvent.[91] The effect of solvent ionization potential on drug degradation can be understood in terms of the solvent's ability to participate in or influence degradation reactions. The ionization potential of a molecule is comparatively lower in the singlet excited state than in the ground state. Hence, it is easier to remove an electron in this state. This phenomenon occurs in the presence of an electron acceptor due to photoionization, particularly in molecules having an anionic state.[47,92]

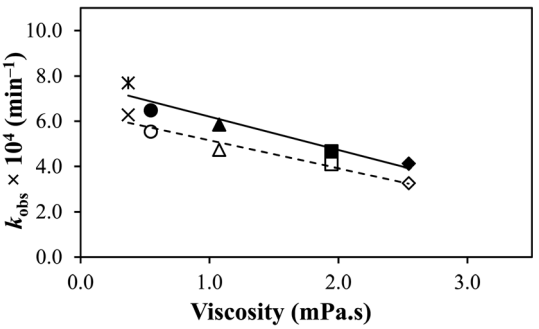

Fig. 6 A plot of k_{obs} of TA *versus* viscosity of the solvents. (*, ×) Acetonitrile, (●, ○) methanol, (▲, Δ) ethanol, (■, □) propanol, and (◆, ◇) butanol. (––––) 2.0×10^4 M; (– – – –) 4.0×10^4 M.

A correlation has been made between the rate constants of TA (Table 2) and the solvents' ionization potential (Table 2). TA and the solvents used in this study possess hydrogen donor and acceptor properties, except for acetonitrile, which only has acceptor ability due to its aprotic nature.[93] Interestingly, a relatively linear relationship (Fig. 7) has been found between the two factors, indicating that the higher the ionization potential of the solvent, the more the degradation of TA, probably due to higher dipole moments and Gibbs energy, as also observed by Faiz *et al.*[94] in a different study.

Effect of solvent density. The solvent density is another parameter that has not been studied much for its impact on drug degradation reactions. Solvent density affects the solute–solvent interactions and alters the relative solvation energies of the reactant and activated complexes, thus affecting the reaction rate.[95] Therefore, another attempt has been made to investigate a correlation between the reaction rates of TA (Table 2) and the solvent densities (Table 2). The results showed that the density of the solvents also plays a vital role in TA degradation since a linear relationship has been found between them in both concentrations (Fig. 8). The solvent with the lowest density (*i.e.*, acetonitrile) showed the maximum photodegradation, while the one with higher density (*i.e.*, 1-butanol) showed comparatively slower degradation (Table 2). This

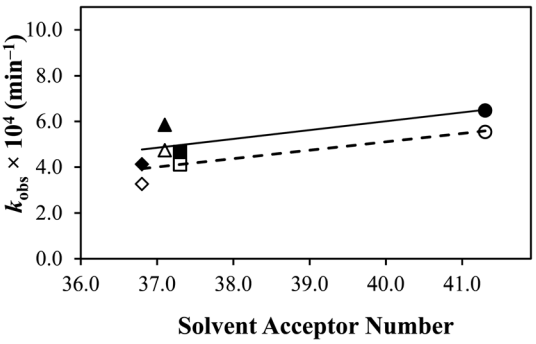

Fig. 5 A plot of k_{obs} of TA *versus* acceptor number of protic solvents (alcohols). (●, ○), Methanol, (▲, Δ) ethanol, (■, □) propanol, and (◆, ◇) butanol. (––––) 2.0×10^4 M; (– – – –) 4.0×10^4 M.

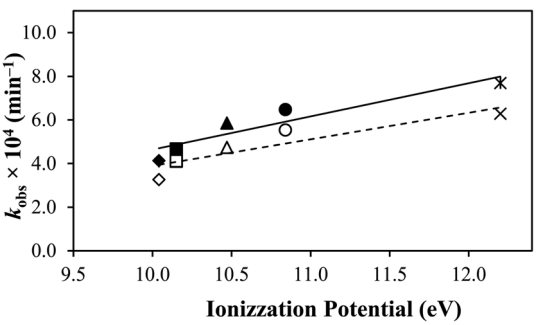

Fig. 7 A plot of k_{obs} of TA *versus* ionization potential of the solvents. (*, ×) Acetonitrile, (●, ○) methanol, (▲, Δ) ethanol, (■, □) propanol, and (◆, ◇) butanol. (––––) 2.0×10^4 M; (– – – –) 4.0×10^4 M.

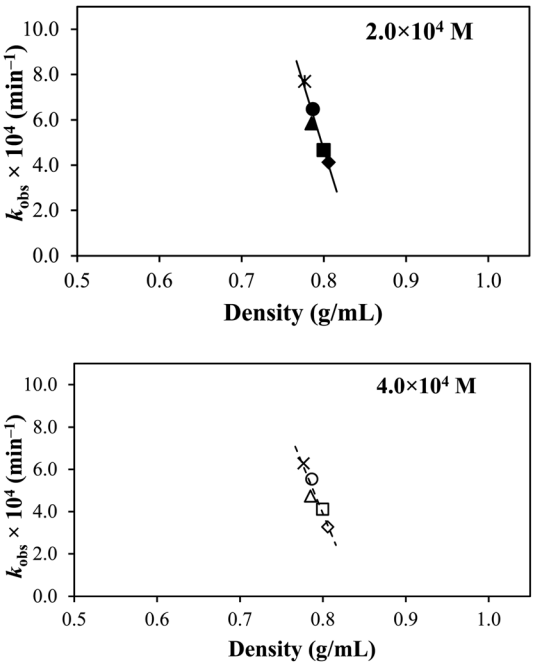

Fig. 8 A plot of k_{obs} of TA *versus* density of the solvents. (*, ×) Acetonitrile, (●, ○) methanol, (▲, Δ) ethanol, (■, □) propanol, and (◆, ◇) butanol.

decrease in photodegradation rates could have happened due to the slower diffusion of reactants or lesser penetration of UV light into the denser solutions, as previously observed for mefenamic acid photodegradation by Shnain *et al.*[90]

Identification of the photodegraded products. The identification of the photoproducts of TA has been made by LC-MS. The chromatograms of TA irradiated for 96 h in different organic solvents are shown in Fig. S11–S15.† Various photoproducts have been identified, and their structures have been proposed with molecular masses (Table 3). Altogether, a total of 17 photoproducts were identified in the photolyzed solutions of TA in different solvents. Of these, only four are common in all solvents (TP-I, XII, XIII, and XVI), while TP-XV and XVII are present in four solvents except ethanol (Table 3). TP-I is identified as 3-chloro-2-methylaniline, the main ingredient used in the synthesis of TA, and is also present as its impurity.[1] Photoproduct TP-IV is found exclusively in 1-butanol, TP-V in ethanol, and TP-VIII in methanol. Thus, the type of solvent and its various physicochemical properties impact not only the reaction rate but also the formation of degradation products, as discussed in the previous sections.

Previously, da Silva *et al.*[29] reported a few photodegradation products of TA by direct photolysis and UV/H_2O_2 process, which are also found in this study, *i.e.*, TP-I till TP-VIII (Table 3). However, in the present study, nine new photoproducts of TA have been identified (TP-IX to TP-XVII) that have not been reported earlier for TA. The formation of different photoproducts in different solvents indicates the impact of the nature of the solvent on the photodegradation of TA.

Degradation of TA in Organic solvents in the dark. A set of similar samples was stored in the dark in a tightly closed container and subjected to HPLC analysis. The samples were observed for any degradation of TA in the organic solvents in the dark at similar time intervals to those of photodegradation studies. No substantial change in the recovery values of TA (100 ± 2%) has been observed for four days (*i.e.*, 96 h) in any solvent, indicating that the light source is the primary catalyst for initiating TA degradation. Previously, Ahmed *et al.*[27] also reported no change in the TA concentration when stored in various organic solvents at room (25 ± 1 °C) and refrigerated (5 ± 3 °C) temperatures for 24 h.

Blank control. The solvents used in this study are known to have a UV cut-off value of ≤220 nm, which means they absorb the UV light at or below this wavelength and not on any other wavelengths.[68,91] However, to ascertain their effect, a set of placebo solvents (*i.e.*, without TA) was irradiated similarly for the same duration as those containing the drug and subjected to HPLC analysis. No change has been observed in any solvent after 96 h of irradiation, indicating the non-reactivity of the solvents. Hence, the photoproducts formed are of TA and not of any solvent.

Mode of photodegradation. Different workers have conducted photostability studies on TA.[29,30] However, there is dearth that no such work has been carried out to evaluate the photostability of TA in aqueous (pH 2.0–12.0) and organic solvents (acetonitrile, methanol, ethanol, 1-propanol, 1-butanol). The viable mechanism for the photodegradation of TA in the aqueous and organic medium is described below.

Aqueous solutions. TA molecule on irradiation is converted into an excited singlet state (^{1}[TA]) (1) which is then converted into an excited triplet state (^{3}[TA]) through intersystem crossing (isc) (2). The ^{3}[TA] state interacts with ground state TA to form anionic and cationic radicals (3). These anionic and cationic radicals may accept or lose a proton, which results in the formation of reduced (4) and oxidized TA radicals (5). The two TAH$^\bullet$ radicals may form oxidized and reduced TA molecules (6). The TA$^\bullet$ may further lead to the formation of degradation products (7).

$$^0[TA] \xrightarrow{h\nu} {}^1[TA] \quad (1)$$

$$^1[TA] \xrightarrow{isc} {}^3[TA] \quad (2)$$

$$^3[TA] + {}^0[TA] \rightarrow TA^{\bullet -} + TA^{\bullet +} \quad (3)$$

$$[TA^{\bullet -}] \xrightarrow{H^+} [TAH^\bullet] \quad (4)$$

$$[TA^{\bullet +}] \xrightarrow{-H^+} [TA^\bullet] \quad (5)$$

$$^2TAH^\bullet \rightarrow TA + TAH_2 \quad (6)$$

$$TA^\bullet \rightarrow \text{degradation products} \quad (7)$$

Table 3 Photoproducts of TA identified by LC-MS in various organic solvents after 96 h of irradiation[a,b]

Compound	Accurate mass	RT	Molecular formula	Proposed structure	ACN	MeOH	EtOH	PrOH	BuOH
TP-I	141.0345	7.0	$C_7H_8Cl_1N_1$	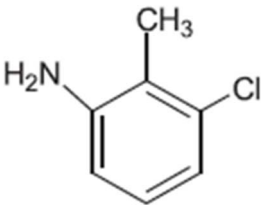	+	+	+	+	+
TP-II	157.0294	6.4	$C_7H_8Cl_1N_1O_1$	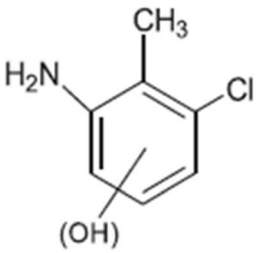		+		+	
TP-III	170.0215	5.5	$C_7H_6O_5$	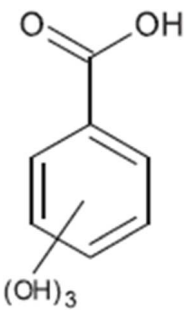		+	+		
TP-IV	224.0532	0.9	$C_7H_{12}O_8$	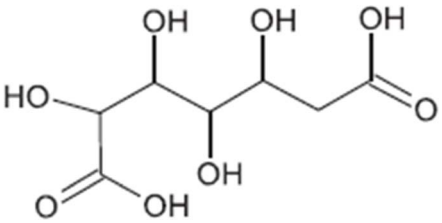					+
TP-V	243.0895	0.7	$C_{14}H_{13}N_1O_3$	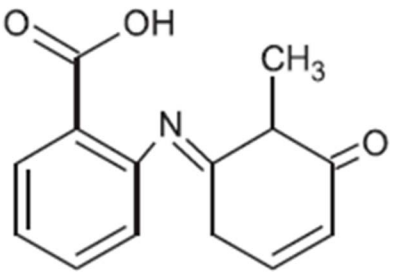			+		
TP-VI	277.0505	7.8	$C_{14}H_{12}Cl_1N_1O_3$	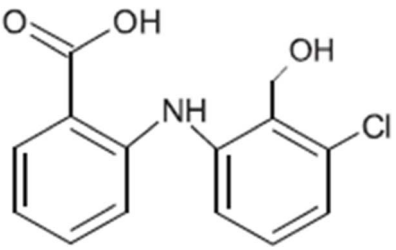		+	+		

Table 3 (*Contd.*)

Compound	Accurate mass	RT	Molecular formula	Proposed structure	ACN	MeOH	EtOH	PrOH	BuOH
TP-VII	295.1055	8.0	$C_{14}H_{17}N_1O_6$	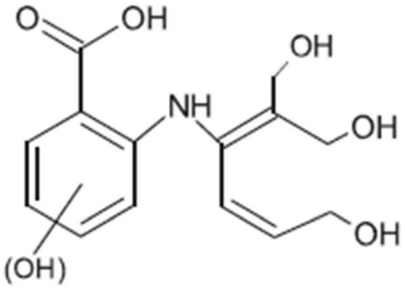		+		+	
TP-VIII	307.0247	7.6	$C_{14}H_{10}Cl_1N_1O_5$	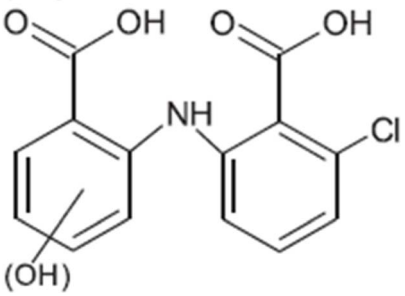		+			
TA	261.0556	9.9	$C_{14}H_{12}Cl_1N_1O_2$	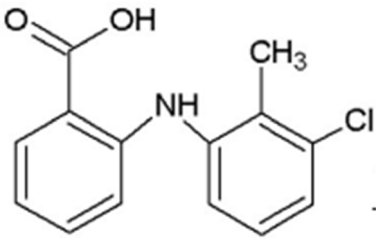	+	+	+	+	+
TP-IX	326.3059	10.9	$C_{20}H_{39}NO_2$	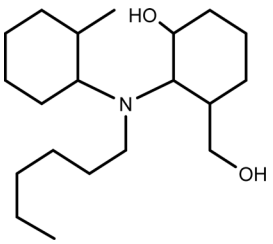		+	+	+	
TP-X	347.2824	10.9	$C_{22}H_{37}NO_2$	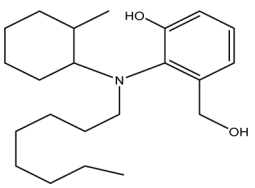		+	+	+	
TP-XI	362.2780	10.9	$C_{18}H_{38}N_2O_5$	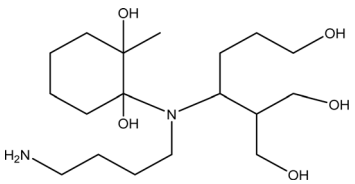		+	+	+	

Table 3 (*Contd.*)

Compound	Accurate mass	RT	Molecular formula	Proposed structure	ACN	MeOH	EtOH	PrOH	BuOH
TP-XII	352.2613	10.7	$C_{21}H_{36}O_4$	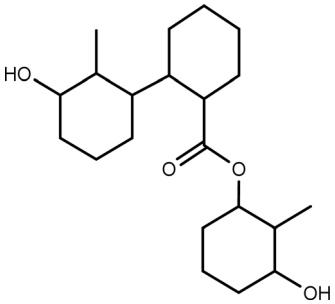	+	+	+	+	+
TP-XIII	320.2311	10.2	$C_{15}H_{32}N_2O_5$	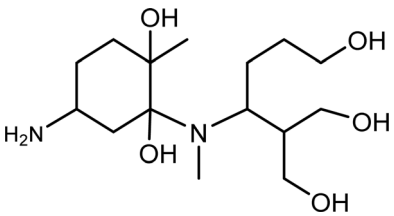	+	+	+	+	+
TP-XIV	242.1518	6.8	$C_{13}H_{22}O_4$	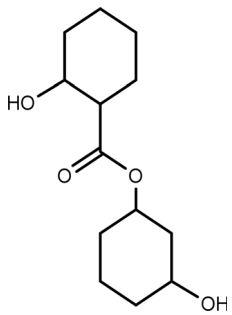		+		+	+
TP-XV	210.0892	7.3	$C_{11}H_{14}O_4$	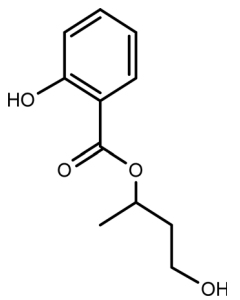	+	+		+	+
TP-XVI	213.0789	8.1	$C_{13}H_{11}N_1O_2$	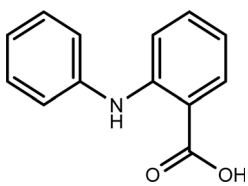	+	+	+	+	+
TP-XVII	240.1725	9.5	$C_{14}H_{24}O_3$	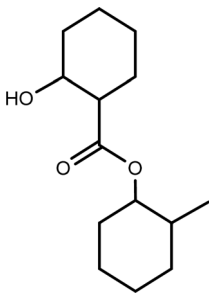	+	+		+	+

[a] ACN = acetonitrile; MeOH = methanol; EtOH = ethanol; PrOH = 1-propanol; BuOH = 1-butanol. [b] The positive sign (+) indicates the presence of the photoproduct in the solvent.

Organic solvents. The triplet state of TA (^{3}[TA]) by interacting with solvent molecules/ions results in the formation of a dipolar intermediate (8). This dipolar intermediate is further converted into the anion ($TAH^{\bullet -}$) and cation ($A^{\bullet +}$) radicals (8). The anion radical on oxidation transforms into the degraded and undegraded TA (9). The reaction scheme showing the involvement of dipolar intermediate in the photolysis of TA in organic solvents results in the degradation of TA is shown in Fig. 9.

$$^3[TA] + AH \xrightarrow{\text{organic solvent}} \underset{\text{dipolar intermediate}}{(TA^{\sigma-}\cdots\cdots H\cdots\cdots A^{\sigma+})} \rightarrow TAH^- + A^{\bullet +} \quad (8)$$

$$TAH^{\bullet} \xrightarrow[\text{photooxidation}]{O_2} \text{undegraded TA} + \text{degradation products} \quad (9)$$

The degradation products identified by LC-MS/MS are given in Table 3. Based on the identification of these products formed during the photolysis reaction in different organic solvents, a photodegradation pathway has been proposed and shown in Fig. 9. TA on the absorption of light undergoes several processes, including ring-cleavage, bond-cleavage, oxidation-reduction, dechlorination, addition and removal of amine, which results in the formation of various photoproducts (Fig. 9). The degree of the formation of these photoproducts is dependent on the nature of the solvent, solvent characteristics, and interaction of TA with the specific solvent molecule.

ESR spectrometric studies. The conversion of the excited singlet state of TA (^{1}[TA]) to the excited triplet state (^{3}[TA]) has been investigated in acetonitrile at room temperature, as depicted in Fig. S16.† The ESR spectra obtained for TA before and after acetonitrile irradiation reveal insights into this photophysical process. Before irradiation, the ESR spectrum showed no significant signal, indicating the absence of the triplet state. However, an ESR signal is observed post-irradiation corresponding to the excited triplet state (^{3}[TA]). This transition suggests that upon irradiation, there is an efficient intersystem crossing from the excited singlet state (^{1}[TA]) to the triplet state (^{3}[TA]). These findings provide compelling evidence that irradiation in acetonitrile induces the conversion of ^{1}[TA] to ^{3}[TA], underscoring the role of the solvent environment and irradiation conditions in modulating the photophysical behavior of TA.

Quantum yields of photolysis. The quantum yields for the photolysis of TA in aqueous (pH 2.0–12.0) and organic solvents (acetonitrile, methanol, ethanol, 1-propanol, 1-butanol) have been calculated (Tables 1 and 2), and the values are in the range of 0.23–2.45 and 0.06–0.18, respectively. These calculated quantum yield values are affected by the pH of the medium and the reactivity of the excited triplet state in aqueous and organic solvents. In the acidic region, the Φ values are higher than those

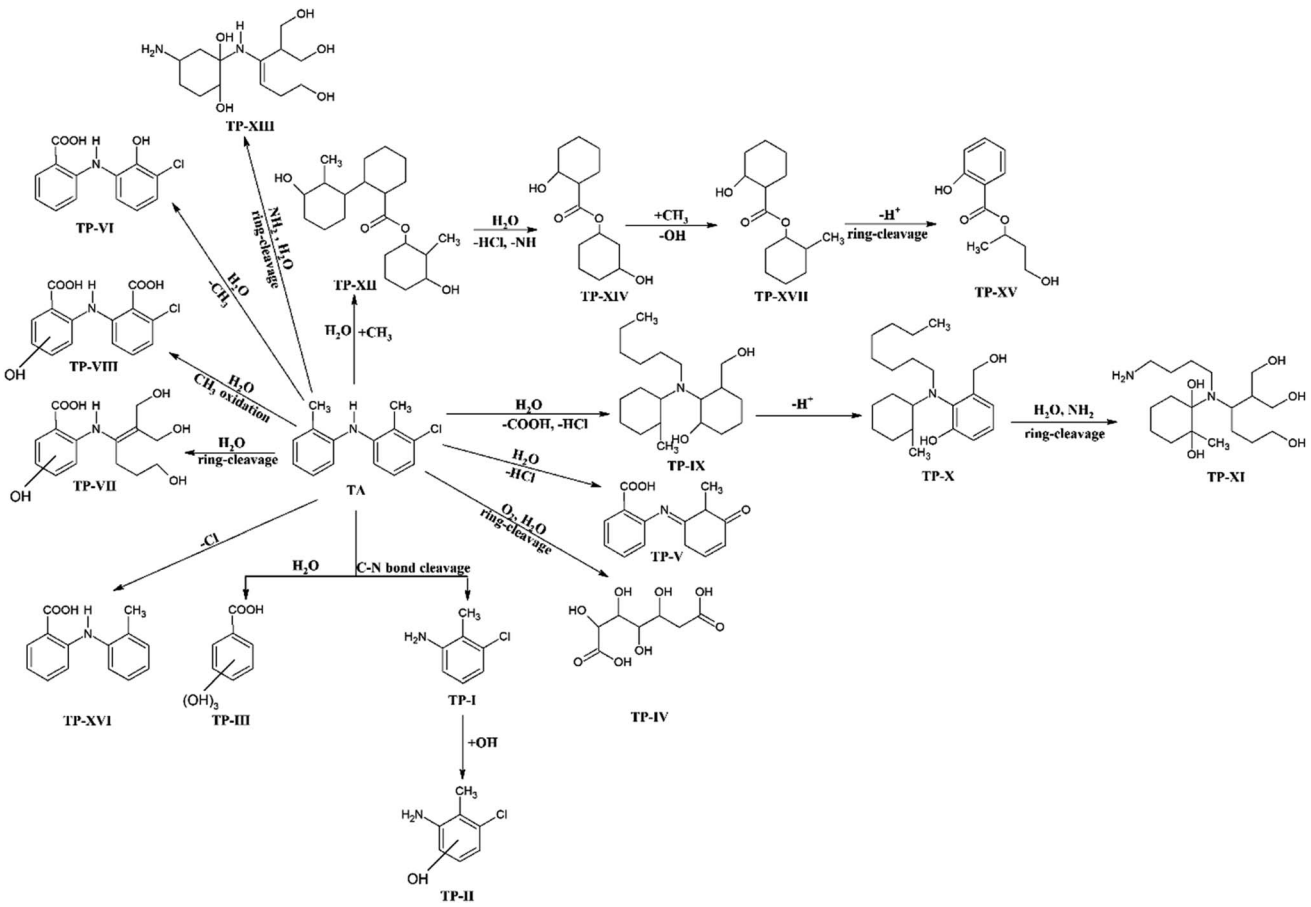

Fig. 9 Suggested photodegradation pathways for the degradation of TA to form various degradation products.

in the alkaline region, indicating that in the case of TA, the high reactivity of the excited triplet state in the acidic region results in the increased photodegradation of TA.

Conclusion

TA is a photosensitive compound that is photolyzed by UV irradiation. The present study is based on the determination of the kinetics of TA in aqueous and organic solvents. The rate–pH profile represents a V-top shape curve, and the rate of degradation increased with an increase in pH from 2.0 to 3.0 (pK_{a1}, 1.95), and beyond 4.0 (pK_{a2}, 4.05), the rates of photodegradation decreased till pH 12.0. The higher rate of TA degradation at acidic pH is due to the sensitivity of TA towards acid hydrolysis, and a decrease in the rates of degradation at higher pH is due to the less susceptibility of TA molecules towards alkaline hydrolysis. The bulk properties of the medium used play an important role in the drug's stability. It has been found that the rate of photolysis of TA increases with the polarity of the medium and decreases with an increase in the medium viscosity.

Conflicts of interest

There are no conflicts to declare.

Note added after first publication

This article replaces the version published on 8 July 2024, in which equations 8 and 9 were labelled incorrectly.

References

1 S. Ahmed, M. A. Sheraz and I. Ahmad, in *Profiles of Drug Substances, Excipients, and Related Methodology*, ed. H. G. Brittain, Academic Press, Elsevier, Cambridge, USA, 2018, vol. 43, pp. 255–319.
2 British National Formulary (BNF) 85, BMJ Group and Royal Pharmaceutical Society, Pharmaceutical Press, London, UK, 2023.
3 J. K. Chang, A. Leso, G. M. Subaiea, A. Lahouel, A. Masoud, F. Mushtaq, R. Deeb, A. Eid, M. Dash, S. W. Bihaqi and N. H. Zawia, *Curr. Alzheimer Res.*, 2018, **15**, 655–663.
4 J. M. Cornejo-Montes-de-Oca, R. Hernández-Soto, A. G. Isla, C. E. Morado-Urbina and F. Peña-Ortega, *Curr. Alzheimer Res.*, 2018, **15**, 731–742.
5 P. Liu, Y. Li, D. Liu, X. Ji, T. Chi, L. Li and L. Zou, *Neurochem. Res.*, 2018, **43**, 1938–1946.
6 A. Leso, S. W. Bihaqi, A. Masoud, J. K. Chang, A. Lahouel and N. Zawia, *Exp. Biol. Med.*, 2019, **244**, 1062–1069.
7 H. Zhang, X. Wang, P. Xu, X. Ji, T. Chi, P. Liu and L. Zou, *J. Physiol. Sci.*, 2020, **70**, 29.
8 J. Hill and N. H. Zawia, *Cells*, 2021, **10**, 702.
9 R. Parveen, B. Sravanthi and P. Dastidar, *Chem.–Asian J.*, 2017, **12**, 792–803.
10 U. T. Sankpal, S. Goodison, M. Jone-Pauley, M. Hurtado, F. Zhang and R. Basha, *Oncotarget*, 2017, **8**, 14593–14603.
11 A. N. Shajahan-Haq, S. M. Boca, L. Jin, K. Bhuvaneshwar, Y. Gusev, A. K. Cheema, D. D. Demas, K. S. Raghavan, R. Michalek, S. Madhavan and R. Clarke, *Oncotarget*, 2017, **8**, 96865–96884.
12 S. Shelake, U. T. Sankpal, W. Paul Bowman, M. Wise, A. Ray and R. Basha, *Invest. New Drugs*, 2017, **35**, 158–165.
13 D. Feldman, E. Leahy and S. H. Lee, *Curr. Med. Chem.*, 2018, **25**, 1598–1608.
14 M. Hurtado, U. T. Sankpal, A. Ranjan, R. Maram, J. K. Vishwanatha, G. P. Nagaraju, B. F. El-Rayes and R. Basha, *Crit. Rev. Oncol. Hematol.*, 2018, **126**, 201–207.
15 M. Hurtado, U. T. Sankpal, A. Kaba, S. Mahammad, J. Chhabra, D. T. Brown, R. K. Gurung, A. A. Holder, J. K. Vishwanatha and R. Basha, *Cell. Physiol. Biochem.*, 2018, **51**, 1894–1907.
16 M. Hurtado, U. T. Sankpal, J. Chhabra, D. T. Brown, R. Maram, R. Patel, R. K. Gurung, J. Simecka, A. A. Holder and R. Basha, *Invest. New Drugs*, 2019, **37**, 27–34.
17 D. Poradowski and B. Obmińska-Mrukowicz, *J. Vet. Res.*, 2019, **63**, 399–403.
18 S. Shelake, U. T. Sankpal, D. Eslin, W. P. Bowman, J. W. Simecka, S. Raut, A. Ray and R. Basha, *Apoptosis*, 2019, **24**, 21–32.
19 J. F. Sun, Y. J. Xu, X. H. Kong, Y. Su and Z. Y. Wang, *Neurosci. Lett.*, 2019, **696**, 67–73.
20 J. Sun, R. Tao, T. Mao, Z. Feng, Q. Guo and X. Zhang, *Toxicol. Appl. Pharmacol.*, 2019, **380**, 114696.
21 M. Hurtado, L. Prokai, U. T. Sankpal, B. Levesque, R. Maram, J. Chhabra, D. T. Brown, R. K. Gurung, A. A. Holder, J. K. Vishwanatha and R. Basha, *Process Biochem.*, 2020, **89**, 155–164.
22 Y. Ma, P. Yu, S. Lin, Q. Li, Z. Fang and Z. Huang, *Pharmacol. Res.*, 2020, **152**, 104499.
23 S. Siraj, A. Kurri, K. Patel, N. Hamby and R. Basha, *Crit. Rev. Oncog.*, 2020, **25**, 355–363.
24 C. X. Yang, L. Xing, X. Chang, T. J. Zhou, Y. Y. Bi, Z. Q. Yu, Z. Q. Zhang and H. L. Jiang, *Mol. Pharm.*, 2020, **17**, 1300–1309.
25 E. Blanco-Paniagua, A. M. García-Lino, D. García-Mateos, A. I. Álvarez and G. Merino, *Chem. Biol. Interact.*, 2021, **345**, 109537.
26 L. Xing, C. X. Yang, D. Zhao, L. J. Shen, T. J. Zhou, Y. Y. Bi, Z. J. Huang, Q. Wei, L. Li, F. Li and H. L. Jiang, *J. Controlled Release*, 2021, **331**, 460–471.
27 S. Ahmed, N. Mustaan, M. A. Sheraz, S. A. Nabi and I. Ahmad, *J. Pharmacol.*, 2015, **2015**, 216249.
28 British Pharmacopoeia and Her Majesty's Stationary Office, *Electronic Version*, London, UK, 2024.
29 L. D. da Silva, R. P. Cavalcante, R. F. Cunha, F. Gozzi, R. F. Dantas, S. C. de Oliveira and A. M. Junior, *Sci. Total Environ.*, 2016, **573**, 518–531.
30 C. A. Davis, P. R. Erickson, K. McNeill and E. M. L. Janssen, *Environ. Sci.: Processes Impacts*, 2017, **19**, 656–665.
31 S. H. Kazi, M. A. Sheraz, S. G. Musharraf, S. Ahmed, R. Bano, F. Haq and Z. Anwar, *Anti-Inflammatory Anti-Allergy Agents Med. Chem.*, 2024, **23**, 52–70.

32 H. H. Tonnesen, in *The Photostability of Drugs and Drug Formulations*, CRC Press, Boca Raton, FL, USA, 2004.
33 N. S. Abdelwahab, N. W. Ali, M. M. Zaki and M. Abdelkawy, *J. Chromatogr. Sci.*, 2015, **53**, 484–4891.
34 ICH Harmonised Tripartite Guideline, Validation of Analytical Procedures: Text and Methodology Q2(R1), *International Conference on Harmonization of Technical Requirements for Registration of Pharmaceuticals for Human Use*, Geneva, Switzerland, 2005.
35 M. A. Sheraz, S. H. Kazi, S. Ahmed, Z. Anwar and I. Ahmad, *Beilstein J. Org. Chem.*, 2014, **10**, 1999–2012.
36 O. Legrini, E. Oliveros and A. M. Braun, *Chem. Rev.*, 1993, **93**, 671–698.
37 C. A. Parker, *Proc. R. Soc. Lond.*, 1953, **A220**, 104–116.
38 C. G. Hatchard and C. A. Parker, *Proc. R. Soc. Lond.*, 1956, **A235**, 518–536.
39 R. K. Gilpin and W. Zhou, *J. Pharm. Biomed. Anal.*, 2005, **37**, 509–515.
40 S. Jabeen, T. J. Dines, S. A. Leharne and B. Z. Chowdhry, *Spectrochim. Acta, Part A*, 2012, **96**, 972–985.
41 S. Ahmed, M. A. Sheraz and I. U. Rehman, *AAPS PharmSciTech*, 2013, **14**, 870–879.
42 S. Ahmed, M. A. Sheraz, C. Yorucu and I. U. Rehman, *Cent. Eur. J. Chem.*, 2013, **11**, 1533–1541.
43 S. Andleeb, S. Ahmed, M. A. Sheraz, Z. Anwar and I. Ahmad, *Luminescence*, 2020, **35**, 1017–1027.
44 J. T. Carstensen, in *Drug Stability Principles and Practices*, ed. J. T. Carstensen and C. T. Rhodes, Marcel Dekker, New York, USA, 2000, pp. 73–84.
45 K. A. Connors, G. L. Amidon and V. J. Stella, in *Chemical Stability of Pharmaceuticals, A Handbook for Pharmacists*, Wiley, New York, USA, 1986.
46 S. Yoshioka and V. J. Stella, *Stability of Drugs and Dosage Forms*, Kluwer Academic/Plenum Publishers, New York, USA, 2000, pp. 139–150.
47 I. Ahmad, Z. Shad, K. Qadeer and R. Bano, *Baqai J. Health Sci.*, 2016, **19**, 3–11.
48 A. S. Kearney and V. J. Stella, *J. Pharm. Sci.*, 1993, **82**, 69–72.
49 B. V. Shetty, R. L. Schowman, M. Slivak and C. M. Riley, *J. Pharm. Biomed. Anal.*, 1992, **10**, 675–683.
50 J. A. Molica, C. R. Rehin, J. B. Smith and H. K. Govern, *J. Pharm. Sci.*, 1971, **60**, 1380–1384.
51 C. M. Won, *Int. J. Pharm.*, 1994, **104**, 29–40.
52 S. G. Jivani and V. J. Stella, *J. Pharm. Sci.*, 1985, **74**, 1274–1282.
53 I. Ahmad, Q. Fasihullah, A. Noor, I. A. Ansari and Q. N. Ali, *Int. J. Pharm.*, 2004, **280**, 199–208.
54 I. Ahmad, Z. Anwar, K. Iqbal, S. A. Ali, T. Mirza, A. Khurshid, A. Khurshid and A. Arsalan, *AAPS PharmSciTech*, 2014, **15**, 550–559.
55 M. Aminuddin, U. Nazim and I. Ahmad, *Indian J. Pharm. Sci.*, 2011, **73**, 387–393.
56 S. Srisantitham, M. Sukwattanasinitt and S. Unarunotai, *Colloids Surf., A*, 2018, **550**, 123–131.
57 K. Zamojc, I. Bylinska, W. Wiczk and L. Chmurzynski, *Int. J. Mol. Sci.*, 2021, **22**, 885.
58 I. Ahmad, Z. Anwar, S. Ahmed, M. A. Sheraz, R. Bano and A. Hafeez, *AAPS PharmSciTech*, 2015, **16**, 1122–1128.
59 W. Gul, F. H. Vaid, A. Faiyaz, Z. Anwar, A. Khurshid and I. Ahmad, *J. Photochem. Photobiol., A*, 2019, **376**, 22–31.
60 F. H. Vaid, W. Gul, A. Faiyaz, Z. Anwar, M. A. Ejaz, S. Zahid and I. Ahmad, *J. Photochem. Photobiol., A*, 2019, **371**, 59–66.
61 I. Ahmad, M. A. Sheraz, S. Ahmed, R. H. Shaikh, F. H. Vaid, S. R. Khattak and S. A. Ansari, *AAPS PharmSciTech*, 2011, **12**, 917–923.
62 I. Ahmad, K. Qadeer, A. Hafeez, S. Zahid and M. A. Sheraz, *J. Photochem. Photobiol., A*, 2017, **332**, 92–100.
63 S. Ahmed, N. Anwar, M. A. Sheraz and I. Ahmad, *Sci. Technol. Dev.*, 2017, **36**, 206–210.
64 I. Ahmad, M. A. Sheraz and S. Ahmed, *Stability of Drugs and Drug Products*, Higher Education Commission, Islamabad, Pakistan, 2017.
65 F. H. Vaid, S. Zahid, A. Faiyaz, K. Qadeer, W. Gul, Z. Anwar and I. Ahmad, *J. Photochem. Photobiol., A*, 2018, **362**, 40–48.
66 I. Ahmad, R. Bano, M. A. Sheraz, S. Ahmed, T. Mirza and S. A. Ansari, *Acta Pharm.*, 2013, **63**, 223–229.
67 I. Ahmad, R. Bano, S. G. Musharraf, S. Ahmed, M. A. Sheraz, M. S. Bhatti and Z. Shad, *AAPS PharmSciTech*, 2014, **15**, 1588–1597.
68 I. Ahmad, R. Bano, S. G. Musharraf, M. A. Sheraz, S. Ahmed, H. Tahir, Q. ulArfeen, M. S. Bhatti, Z. Shad and S. F. Hussain, *J. Photochem. Photobiol., A*, 2015, **302**, 1–10.
69 J. J. Werner, K. McNeill and W. A. Arnold, *Chemosphere*, 2005, **58**, 1339–1346.
70 P. Chen, W. Lv, Z. Chen, J. Ma, R. Li, K. Yao, G. Liu and F. Li, *Environ. Sci. Pollut. Res. Int.*, 2015, **22**, 12585–12596.
71 P. Chen, F. L. Wang, K. Yao, J. S. Ma, F. H. Li, W. Y. Lv and G. G. Liu, *Bull. Environ. Contam. Toxicol.*, 2016, **96**, 203–209.
72 R. Colombo, T. C. Ferreira, R. A. Ferreira and M. R. Lanza, *J. Environ. Manage.*, 2016, **167**, 206–213.
73 Y. F. Velazquez and P. M. Nacheva, *Environ. Sci. Pollut. Res. Int.*, 2017, **24**, 6779–6793.
74 J. Li, H. Zhou, R. Chen, T. Yu and M. Ye, *J. Adv. Oxid. Technol.*, 2017, **20**, 20160188.
75 M. Nabeel, Thermal Stability of Tolfenamic Acid in Liquid Media, *Master of Philosophy thesis*, Baqai Medical University, 2017.
76 B. Kaushik, G. Rao and D. Vaya, Photocatalytic degradation of drugs, in *Handbook of Green and Sustainable Nanotechnology*, ed. U. Shanker, C. M. Hussain and M. Rani, Springer Nature, Switzerland, 2022, pp. 1–29.
77 F. Madjene and N. Yeddou-Mezenner, *Sep. Sci. Technol.*, 2018, **53**, 364–373.
78 I. Ahmad, T. Mirza, S. G. Musharraf, Z. Anwar, M. A. Sheraz, S. Ahmed, M. A. Ejaz and A. Khurshid, *RSC Adv.*, 2019, **9**, 26559–26571.
79 S. U. Khattak, D. Shaikh, I. Ahmad, K. Usmanghani, M. A. Sheraz and S. Ahmed, *AAPS PharmSciTech*, 2013, **14**, 177–182.
80 M. A. Sheraz, S. H. Kazi, S. Ahmed, T. Mirza, I. Ahmad and M. P. Evstigneev, *J. Photochem. Photobiol., A*, 2014, **273**, 17–22.

81 A. Khurshid, I. Ahmad, N. Khan, M. Usmani and Z. Anwar, *Int. J. Chem. Kinet.*, 2023, **55**, 190–203.
82 E. R. Garrett, *J. Pharm. Sci.*, 1962, **51**, 811–833.
83 I. Racz, *Drug Formulation*, John Wiley & Sons, Chichester, UK, 1989, p. 128.
84 P. Sinko, Chemical Kinetics and Stability, *Martin's Physical Pharmacy and Pharmaceutical Sciences*, Lippincott Williams & Wilkins, Philadelphia, USA, 2017, ch. 14.
85 Z. Peng, L. HaiXia, Y. SiDe and W. WenFeng, *Sci. China Chem.*, 2014, **57**, 409–416.
86 M. A. Sheraz, M. F. Khan, S. Ahmed, S. H. Kazi, S. R. Khattak and I. Ahmad, *Int. J. Cosmet. Sci.*, 2014, **36**, 494–504.
87 K. J. Laidler, *Chemical Kinetics*, Pearson Education, New Delhi, India, 3rd edn, 1987.
88 A. Pross, *Theoretical & Physical Principles of Organic Reactivity*, John Wiley & Sons, Inc., New York, USA, 1995.
89 A. A. Alwasiti, Z. Y. Shnain, M. F. Abid, A. A. Razak, B. A. Abdulhussein and G. S. Mahdi, *Earth Sci. Environ.*, 2021, **779**, 012073.
90 Z. Y. Shnain, M. F. Abid and K. A. Sukkar, *Desalination Water Treat.*, 2021, **210**, 22–30.
91 W. M. Haynes, *CRC Handbook of Chemistry and Physics*, CRC Press, Bocca Raton, FL., USA, 2017.
92 S. Navaratnum, Photochemical and photophysical methods used in the study of drug photoreactivity, in *The Photostability of Drugs and Drug Formulations*, ed. H. H. Tonnesen, Taylor & Francis, London, UK, 2004, pp. 255–284.
93 National Center for Biotechnology Information, PubChem Compound Summary for CID610479, Tolfenamic acid, **https://pubchem.ncbi.nlm.nih.gov/compound/Tolfenamic-acid**, last accessed april 30, 2024.
94 M. R. Faiz, D. Widhiyanuriyawan, E. Siswanto and I. N. Wardana, *IOP Conf. Ser.: Mater. Sci. Eng.*, 2018, **299**, 012089.
95 S. C. Tucker and M. W. Maddox, *J. Phys. Chem. B*, 1998, **102**, 2437–2453.